High-order harmonic generation in rare gases with subpicosecond XeCl laser pulses

Kenzo Miyazaki, Hirofumi Sakai, Gyu Ug Kim,* and Hideyuki Takada
Laser Section, Optoelectronics Division, Electrotechnical Laboratory, 1-1-4, Umezono, Tsukuba 305, Japan
(Received 16 November 1992; revised manuscript received 17 February 1993)

A systematic study of the high-order harmonic generation in He, Ne, Ar, Kr, and Xe has been made using subpicosecond XeCl laser pulses at a maximum laser intensity of 3.5×10^{15} W/cm^2. The highest orders of harmonics observed are the 15th in He, the 13th in Ne, and the 9th in Ar, Kr, and Xe, and no broad plateau is formed in the harmonic distributions. The ultraviolet laser pulse, which has a large multiphoton ionization rate, was observed to induce a strong dielectric breakdown of the nonlinear medium at the high intensity. Multiphoton ionization and the subsequent dielectric breakdown of the medium are shown to have a significant influence on the harmonic-generation processes, as well as on the harmonic distribution. The laser-wavelength dependence of the high-order harmonic generation is discussed by comparing the results with those obtained by the subpicosecond visible dye-laser pulses.

PACS number(s): 42.65.Ky, 42.50.Hz, 32.80.Rm

I. INTRODUCTION

Developments of intense ultrashort-pulse lasers have made it possible to produce light intensities of $10^{14}-10^{18}$ W/cm^2. At this laser intensity, the high-frequency radiation field generated becomes comparable to or in excess of the typical atomic Coulomb field of 10^8-10^9 V/cm. Recently, much attention has been focused on the high-order harmonic generation with such ultrashort-pulse, high-brightness lasers, because the results have suggested a new domain of nonlinear optics at an intense radiation field and provided a promising approach to developing useful coherent vacuum-ultraviolet (VUV) to soft-x-ray radiation sources. The high-order harmonic generation has been done in gaseous mediums at different fundamental wavelengths of Nd:YAG (where Nd:YAG denotes neodymium-doped yttrium-aluminum-garnet) [1], Nd:glass (1053 and 526 nm) [2–4], KrF (248 nm) [5,6], dye (616 nm) [7], and Ti: sapphire (806 nm) [8] lasers. The highest-order of harmonic radiation observed so far is the 135th of a ps Nd:glass laser at 1053 nm [3], and the shortest-wavelength harmonic generated is 7.4 nm, which is the 109th-order harmonic observed in Ne with fs Ti:sapphire (806 nm) laser pulses [8].

The experimental results reported so far have represented significant dependences of the high-order harmonic generation on the laser wavelength. For example, one of the most characteristic behaviors of high-order harmonic radiation observed is a *plateau* in the harmonic distributions where the intensities of successive harmonics are within a range of an order of magnitude. Typical harmonic distributions including a broad plateau have been observed by ps Nd:YAG [1] and glass [2,3], sub-ps dye [7], and fs Ti:sapphire [8] lasers, where the highest order of harmonic detected appears to increase with increasing laser wavelength. The plateau formation in a harmonic distribution was first pointed out in the experiment using ps KrF laser pulses [5]. The results obtained by the ultraviolet (UV) lasers [5,6], however, do not represent such a *broad* plateau as observed with the infrared and visible lasers, and the highest order of harmonic obtained at the UV is the 25th of a KrF laser [6], despite the high UV laser intensities used in the experiments. Such a wavelength dependence of the high-order harmonic generation is not understood completely and is still one of the most essential subjects to be studied for the new domain of nonlinear optics associated with the breakdown of conventional radiative perturbation theory and for the development of coherent short-wavelength radiation sources.

In the previous paper [7] (hereafter referred to as I), the present authors have presented the experimental results of high-order harmonic generation obtained with the sub-ps dye (616-nm) laser pulses and discussed the role of the ac Stark effect in the high-order harmonic generation at high intensities. This paper reports a series of experimental results of high-order harmonic generation in He, Ne, Ar, Kr, and Xe with sub-ps XeCl (308-nm) laser pulses. We have concentrated our attention on the characteristic effects of intense UV pulses on the high-order harmonic generation, especially those associated with the ionization and subsequent dielectric breakdown of the medium. For this, most experiments have been made using UV intensities much higher than the saturation intensity for multiphoton ionization (MPI) of atoms, as well as for the purposes of simulating the KrF laser experiments [5,6] and studying the possible contribution of ions to the harmonic generation that was recently shown theoretically [9,10]. In what follows we describe the experimental apparatus and procedure. In Sec. III, the results are presented, and the harmonic distributions observed in He, Ne, Ar, Kr, and Xe are discussed, as well as the role of the ac Stark effect on the harmonic generation in the UV, and the influence of multiphoton ionization and subsequent dielectric breakdown of the nonlinear medium. The experimental results obtained by the UV

*Permanent address: Korea Research Institute of Science and Technology, P.O. Box 3, Taedok Science Town, Taejon 305-606, Korea.

laser are also compared with those obtained by the visible dye laser.

II. EXPERIMENT

A. Laser system

The sub-ps UV radiation was produced using a commercial (Spectra Physics) dye-laser oscillator-amplifier system, described in I. The arrangement of the whole laser system, including two excimer laser amplifiers, is schematically shown in Fig. 1. The master oscillator is a cw mode-locked Nd:YAG laser producing 100-ps pulses. The laser pulses are compressed to a few ps by a fiber-grating compressor and frequency doubled in a potassium titanyl phosphate (KTP) crystal. The 532-nm pulses pump a synchronously-mode-locked linear-cavity dye laser, which produces ~500-fs pulses. The central wavelength of the dye-laser output is tuned to 616 nm. The dye-laser pulses are compressed to ~100 fs by a fiber-prism compressor and directed to the three-stage amplifiers. Simultaneously, a small portion of the master oscillator output is amplified by a regenerative Nd:YAG laser amplifier operating at 10 Hz. A single amplified 100-ps pulse is extracted from the regenerative amplifier and further amplified by a Nd:YAG laser power amplifier. This output is frequency doubled, and the 50-mJ green pulse pumps the three-stage dye-laser amplifiers. The visible dye-laser output is 2 mJ in 800-fs [full width at half maximum (FWHM)] pulses, having a spectral bandwidth of 1.3 nm. The time-bandwidth product is 2–3 times larger than the transform-limited value for a sech^2 and/or Gaussian pulse. This is due most probably to unavoidable phase modulation that is introduced in the three-stage amplifiers. The harmonic-generation experiments in the visible were made using the dye-laser output.

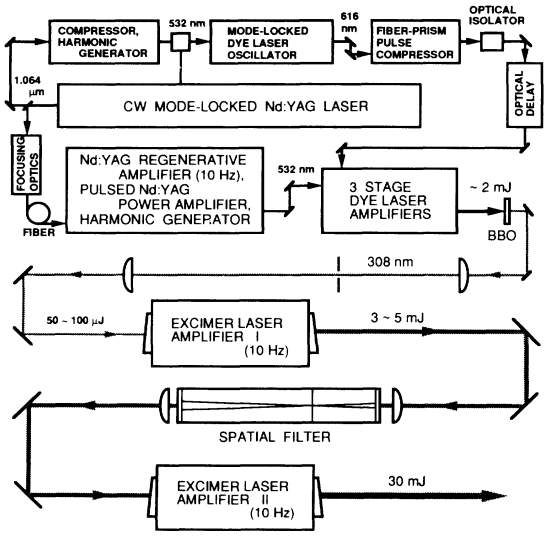

FIG. 1. Experimental arrangement of the subpicosecond XeCl laser amplification system. The UV laser is based on a sub-ps dye-laser oscillator-amplifier system of which output wavelength is tuned to 616 nm. BBO denotes a β-BaB_2O_4 crystal.

For production of the UV pulses, the 616-nm dye-laser output is frequency doubled in a 0.5-mm-thick β-BaB_2O_4 crystal. The 308-nm radiation is separated from the visible by a dichroic mirror and spatially filtered with a 0.2-mm-diameter aperture. The UV seed pulse of about 50–100 μJ is amplified in a discharge XeCl excimer laser [amplifier I (Questek 2820)] having tilted windows. The amplified pulse energy was 3–5 mJ in a beam size of 1×1 cm^2. The output beam from amplifier I is spatially filtered with a 0.1-mm-diameter diamond aperture set in vacuum and is enlarged to match with the 2×2-cm^2 discharge cross section of the second XeCl laser amplifier (amplifier II). Amplifier II is a homemade excimer laser of which design, operation, and ps-pulse amplification characteristics have been described in detail elsewhere [11]. The incident 3–5-mJ pulse energy was large enough to saturate the amplifier II gain to produce the amplified pulse energy of 30 mJ at a repetition rate of 10 Hz.

The UV laser-pulse widths were reliably measured with the background-free autocorrelation method using the third- and fifth-harmonic generation in a rare-gas jet. This technique for the UV pulse-width measurement was developed recently by the present authors [12]. We observed pulse-width narrowing in successive amplification. The measured pulse widths were 380 fs for the amplifier I output and 340 fs or less for amplifier II, assuming a sech^2 shape. The time-bandwidth product is about two times larger than the transform-limited value for the XeCl laser. Generation of shorter UV pulses or the transform-limited pulses may require suppression or compensation of the self-phase modulation introduced in the dye-laser amplifiers.

B. Apparatus for the harmonic generation

The experimental arrangement for the harmonic generation is shown in Fig. 2. The linearly polarized UV or dye-laser output is focused with a CaF_2 lens into a supersonic rare-gas beam that is provided from a pulsed gas valve (Lasertechnics LPV) having a modified nozzle of 1-mm diameter. The focusing lengths of the lens were 144 mm for the XeCl laser and 150 mm for the dye laser. The spot size of the focused laser beam was estimated from the measured beam divergence and the focal length of the lens and also from the measured focal profile. Depending on the beam divergence adjustment, the confocal parameters for the focused XeCl and dye-laser beams were $b=3.7$–4.5 and 8.0–8.2 mm, respectively. The confocal parameters are much larger than the interaction length of 1 mm, which may improve the phase-matching condition for the high-order harmonic generation [13,14].

The focused laser intensity I was deduced from the measured pulse energy, the focal area, and the pulse width. The uncertainty in I was less than a factor of 2. The maximum value of I used for the harmonic generation was 3.5×10^{15} W/cm^2 with the XeCl laser and 2×10^{14} W/cm^2 with the dye laser. For the experiments at different laser intensities, the UV and visible laser outputs were varied using a polarizer coupled with a half-wave plate.

The XeCl laser system could produce $I\sim3\times10^{16}$

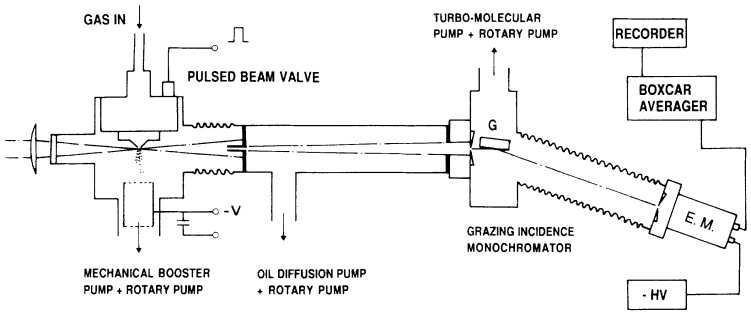

FIG. 2. Experimental arrangement for the harmonic generation. E.M., Electron multiplier; G, Grating.

W/cm^2. In the harmonic generation, however, the fundamental UV intensity had to be reduced by about an order of magnitude because of the extremely strong dielectric breakdown of the medium, which greatly restricted efficient harmonic generation. Furthermore, the UV laser intensity of more than $I \sim 3\times10^{15}$ W/cm^2 did not improve the high-order harmonic-generation properties and was observed to give a worse signal-to-noise ratio of the harmonic signal. Therefore most of the UV laser experiments were made using the amplifier II output.

In the downstream of the atomic beam, as shown in Fig. 2, a simple charge collector is placed for detecting ions that are produced through MPI and subsequent dielectric breakdown of the nonlinear medium. To avoid the effect of amplified spontaneous emission (ASE) from amplifier I or II on the experiments, the harmonic-generation apparatus was placed ~ 5 m apart from the output windows of the excimer laser amplifiers. We confirmed that the weak ASE included in the amplified UV pulse never produced a detectable MPI signal in the gas jet.

The backing gas pressure was fixed for each kind of rare gas throughout the present experiments, and the number density in the interaction region was estimated numerically [15] from the backing pressure and the nozzle configuration to be 4.0×10^{18} cm^{-3} for He, 2.7×10^{18} cm^{-3} for Ne, and 4.3×10^{17} cm^{-3} for Ar, Kr, and Xe.

The harmonic radiation generated in the spectral region of less than $\lambda \approx 70$ nm was detected by a windowless Cu-BeO electron multiplier (Hamamatsu R595) mounted on a 1-m grazing incidence monochromator (Minuteman 310-G) with an Au-coated 600-grooves/mm grating. For the harmonic radiation of $\lambda \approx 35-210$ nm, we used another 20-cm focal length VUV monochromator (Acton VM-502) having an Ir-coated 1200-grooves/mm grating, and an electron multiplier and a solar-blind CsI photomultiplier were attached on each of two exit slits of the monochromator. The harmonic signals detected are processed with a boxcar averager and recorded on a chart recorder.

In order to know the relative harmonic signal, we made a careful calibration for the wavelength dependence of detection sensitivity over the spectral region concerned. We used a theoretical diffraction efficiency for the Au-coated grating [16] and the manufacturers' calibration curves for the Ir-coated grating and light detectors. The wavelength dependence of detection sensitivity obtained was compared with that of a similar VUV–soft-x-ray detection system [17], which was calibrated using a synchrotron radiation facility in our laboratory. Both were in agreement within 50%.

III. RESULTS AND DISCUSSION

A. Harmonic distributions

An example of the harmonic spectrum observed in He with the XeCl laser is shown in Fig. 3. The highest order of harmonic radiation observed with the UV is the 15th (20.5 nm) in He, the 13th (23.7 nm) in Ne, and the 9th (34.2 nm) in Ar, Kr, and Xe. The harmonic signal was much larger than that with the visible laser pulses for the identical nonlinear medium when the comparison was made for approximately the same wavelength region, whereas the UV laser intensity I used was much higher than that of the visible. At $I \sim 3\times10^{15}$ W/cm^2, strong dielectric breakdown was observed for all the rare gases used, but neither intense line emission nor large background continuum was observed, as can be seen in Fig. 3.

Figure 4 shows the calibrated harmonic distributions (a) in He and Ne, and (b) in Ar, Kr, and Xe at $I=(2.5-3.1)\times10^{15}$ W/cm^2. It is noted that the most intense harmonic signal in He is observed at the seventh, which is generated near the energy region of the ionization limit (IL). The higher-order harmonics decrease monotonically with an increase in the harmonic order. In the harmonic distribution, a plateaulike structure is formed from the third to the 13th, where the intensities of successive harmonics are within an order of magnitude. The high-order ($\geq$ 5th) harmonics are comparable with or exceed the lowest (third-order) in intensity. This

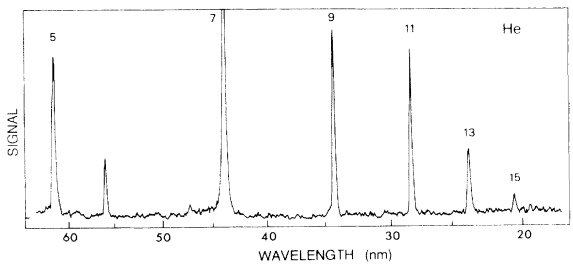

FIG. 3. Example of the high-order harmonic spectrum observed in He at the XeCl laser intensity $I=2.5\times10^{15}$ W/cm^2 with the grazing-incidence monochromator. The spectral peaks are labeled by the harmonic order, whereas the unmarked peaks are the second-order diffractions from the grating.

unusual observation may result from some enhancement of specific harmonics at high intensity, as discussed later. A similar distribution is observed in Ne, and the seventh-order harmonic produced near the IL region is also appreciably enhanced to form a plateaulike structure from the third to the 11th. In Ar, Kr, and Xe, only monotonic decreases in the higher-order harmonics are observed, as shown in Fig. 4(b).

In Fig. 4, no *broad* plateau is formed above the IL, in contrast to those observed by the visible dye laser (see Fig. 2 in I). Furthermore, the highest order of harmonics observed in each rare gas is much less than that observed with the visible laser pulses, as well as the largest harmonic energy produced in He, Ne, and Ar, although I is larger than that of the dye laser by an order of magnitude.

To see in detail the characteristic harmonic-generation property with the UV laser pulses, we measured the harmonic distributions for an increase in I; the results for He and Ne are shown in Figs. 5(a) and 5(b), respectively. At $I<2\times10^{14}$ W/cm^2, only the third-, fifth-, and seventh-order harmonics are observed in He. Note that $I\approx2\times10^{14}$ W/cm^2 is the highest dye-laser intensity used

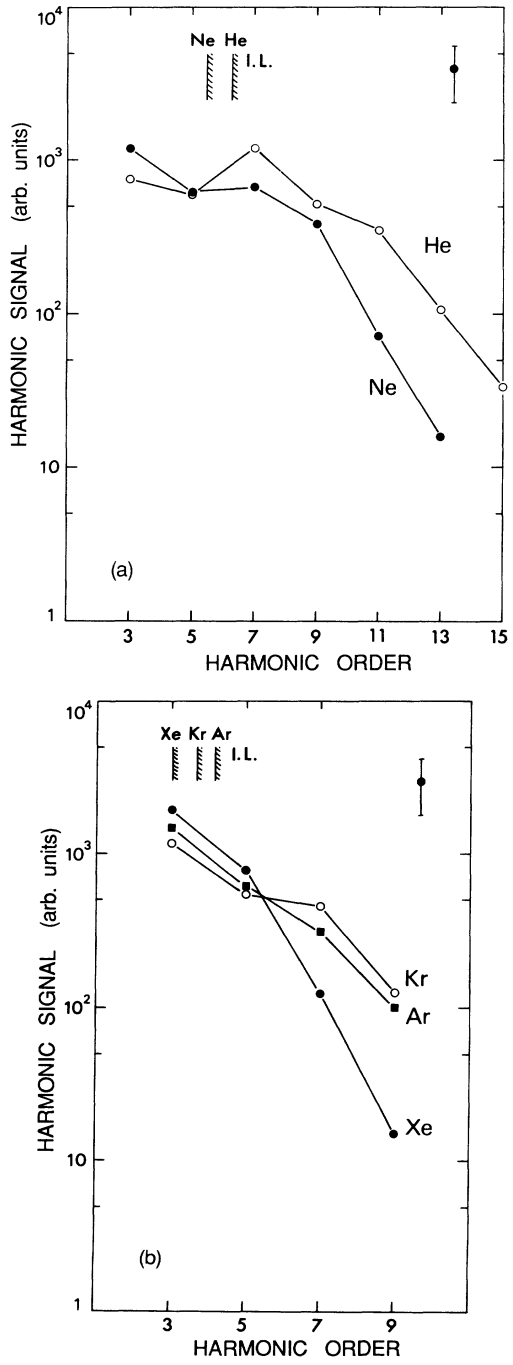

FIG. 4. Harmonic distributions observed in (a) He at $I=2.5\times10^{15}$ W/cm^2 and Ne at $I=2.8\times10^{15}$ W/cm^2, and (b) Ar, Kr, and Xe at $I=3.1\times10^{15}$ W/cm^2 with the XeCl laser pulses. IL denotes the ionization limit.

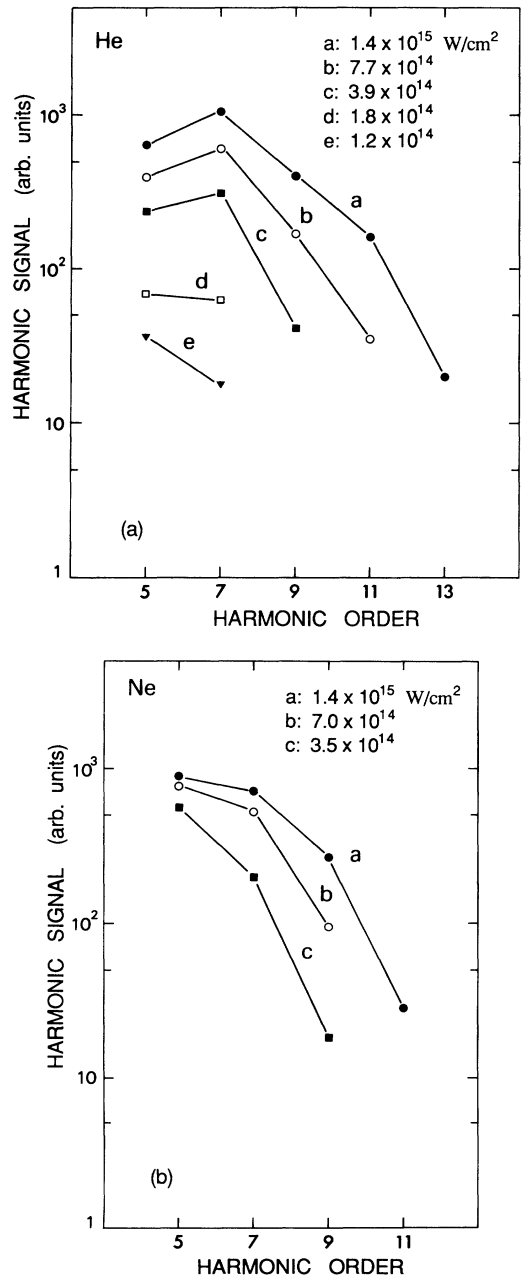

FIG. 5. Harmonic distributions for (a) He and (b) Ne at several XeCl laser intensities.

in I. This certainly shows an advantage of the visible or longer-wavelength laser pulses for generating the higher-order harmonics when I is the same. With an increase in I, the seventh harmonic increases rapidly to overcome the fifth. However, the harmonic distribution having a peak at the seventh is maintained with a further increase in I, while harmonic intensity at each order increases with an increase in I. Similar behavior of harmonic distribution is also observed in Ne, as shown in Fig. 5(b). This is in contrast to the I-dependent harmonic distribution observed with the visible dye-laser pulses. In the dye-laser experiments [7], the successive order of harmonics was greatly enhanced with an increase in I to form a broad plateau.

B. Effect of MPI and dielectric breakdown

The results shown in Fig. 5 suggest that the effective interaction intensity for the high-order harmonic generation was greatly restricted by the medium ionization, as discussed briefly in I. The effect of ionization was confirmed by the simultaneous measurement of harmonic and ion signals as a function of the position of laser focus by translating the focusing lens along the optic axis. An example of the results for He is shown in Fig. 6, where the abscissa is scaled by the relative lens position and the laser pulse propagates from the left to the right. (The accurate focus position in the atomic beam was rather difficult to identify.) Similar measurements of harmonic radiation were made recently by Balcou and co-workers [2,18] using ps Nd:YAG and glass lasers, and the phase-matching effect or the propagation effect of the laser beam on the harmonic generation has been discussed in detail [14,18]. The present experiment provides the first simultaneous measurement of harmonic and ion signals as a function of the laser focus.

At the low laser intensity $I=1.1\times10^{14}$ W/cm^2 in Fig. 6, the fifth-harmonic signal represents a single maximum when the laser pulse is focused into the He beam, as expected. However, at $I=3.4\times10^{15}$ W/cm^2, the harmonic signal exhibits two peaks that are produced by the defocused laser beam. A dip of the harmonic signal is formed when the laser pulse is focused in the He beam region where the ion signal is maximized. The high laser intensity used would greatly exceed the saturation intensity I_s for the MPI of He atoms, as discussed below. Then the result measured as a function of the laser focus should reveal predominantly the effect of medium ionization on the harmonic generation rather than that of phase matching [18].

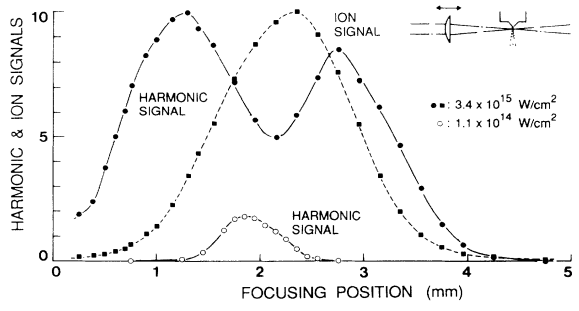

FIG. 6. The fifth harmonic and ion signals in He as a function of position of the XeCl laser focus at $I=3.4\times10^{15}$ W/cm^2 (solid circle and square) and $I=1.1\times10^{14}$ W/cm^2 (open circle). The maximum harmonic and ion signals are normalized to 10. The confocal parameter $b=4.5$ mm.

The same measurements as shown in Fig. 6 were made for the different orders of harmonic radiation and for different mediums. At the highest intensity ($I\sim3\times10^{15}$ W/cm^2), the dip of the harmonic signal was always observed when the incident laser pulse was focused into the beam region, together with the two peaks for the defocused laser beam. It is clear that the reduction of harmonic-generation efficiency in the beam region is due to the ionization of medium or the depletion of neutral atoms.

From Fig. 5(a), one can deduce the maximum laser intensity I_m interacting with He atoms. The result shows that the increase of I to $>3.9\times10^{14}$ W/cm^2 leads to only a relatively small increase in the harmonic signal at each order, maintaining the harmonic distribution, which has the peak at the seventh. If I_m is increased with increasing I ($\gtrsim3.9\times10^{14}$ W/cm^2), the harmonic distribution should be modified by the rapid increase in intensity of the higher-orders. Thus we may conclude that $I_m\sim4\times10^{14}$ W/cm^2, and that the small increase in the harmonics with a further increase in I results from the simultaneous increase in the effective volume of the He beam which interacts at $\sim I_m$. This is certainly expected from the result shown in Fig. 6: at $I=3.4\times10^{15}$ W/cm^2, the incident laser pulse defocused from the He beam region has a larger interaction volume and is still intense enough for the efficient harmonic generation.

The maximum interaction intensity $I_m\sim4\times10^{14}$ W/cm^2 would be close to the saturation intensity I_s for the MPI of He atoms. Although we do not find any published value of I_s for He atoms for 308-nm radiation, one may refer to the results of MPI rates for He at several wavelengths. The calculated rates given by Krause, Schafer, and Kulander [9] lead to $I_s\sim4\times10^{14}$ and $\sim6\times10^{14}$ W/cm^2 for the 0.4-ps 248-nm, and 527-nm laser pulses, respectively. These values suggest that $I_s\sim4\times10^{14}$ W/cm^2 is a reasonable value for the present 0.38-ps 308-nm laser pulse.

We consider the highest order of harmonics to be observed at the UV laser intensity $I_s\sim4\times10^{14}$ W/cm^2. Recently, the simple relation

$$E_{\max}\approx I_p+3E_p \tag{1}$$

was found theoretically by Krause, Schafer, and Kulander [9]. This relation gives the maximum harmonic energy $E_{\max}$ in a plateau, where I_p is the ionization potential of an atom and E_p is the ponderomotive potential given by

$$E_p\sim e^2E_0^2/4m\omega^2\ , \tag{2}$$

with the peak electric field E_0 of a laser pulse at frequency ω, and the electron mass m and charge e. For the present experiment in He, this relation gives $E_{\max}\sim35.2$ eV or the possible harmonic generation up to the ninth

order in a plateau at $I_s \sim 4\times10^{14}$ W/cm^2. The theoretical prediction appears to be consistent with the present observation, as shown in Figs. 4(a) and 5(a).

On the other hand, Krause, Schafer, and Kulander [9] and Xu, Tang, and Lambropoulos [10] have also shown that the highest-order harmonic generated by neutral He atoms is limited up to the 13th at the saturation intensity $I_s=(5-6)\times10^{14}$ W/cm^2 for the 285-fs KrF (248-nm) laser pulses. (Since these theoretical results were in contradiction to the experimental results [6], the theories have proposed and shown the idea that He ions contributed to the higher-order harmonic generation observed.) The calculated results for the KrF laser, as well as the empirical formula given by Eq. (1), suggest that the 15th is a reasonable highest harmonic order that can be generated by neutral He atoms when the effective interaction laser intensity is limited to $I \sim 4\times10^{14}$ W/cm^2.

The highest laser intensity used in the above experiments is larger than I_s by an order of magnitude, but we did not observe any indication of ion contribution to the high-order harmonic generation. This is certainly due to the strong dielectric breakdown which was always observed, even in He at the highest intensity. (The dielectric breakdown may be defined as an avalanche increase in charged particles due to electron collisions and can be deduced from the appearance of a visible light flash in a gaseous medium [19]. In the present experiments, the breakdown is induced by the free electrons produced through the MPI.) Although we could not measure the accurate threshold intensity for the breakdown, the experimental results shown above suggest that the saturation of MPI readily induced the breakdown of He. In fact, we observed the visible light flash due to the breakdown of He at $I \gtrsim 4\times10^{14}$ W/cm^2.

Once the breakdown takes place in the medium, one can hardly expect an ion contribution to the harmonic generation. Dielectric breakdown brings about a large and random dissipation of the laser energy into the medium [19] and would terminate the coherent interaction of the laser pulse with the atomic medium. When a high-density atomic medium is irradiated by a relatively long laser pulse, the breakdown is often induced before the saturation of MPI, and then the effective interaction intensity for the harmonic generation is limited in the medium to a much lower value than that used or expected. Since the breakdown threshold is approximately inversely proportional to the laser-pulse duration, the laser-pulse width has to be as short as possible to increase the interaction intensity up to I_s in the nonlinear medium.

On the other hand, when the peak intensity is much larger than I_s, the *instantaneous* laser intensity which interacts with neutral atoms can exceed I_s before the complete depletion of atoms. Moreover, if the dielectric breakdown proceeds more slowly than the temporal evolution of an intense ultrashort laser pulse, the incident laser pulse can interact even with ions produced through the MPI. These competitive interaction processes strongly depend on the laser intensity, the laser-pulse width (and shape), and the medium density. In addition to the expansion of effective interaction volume discussed above, the fast rise time of an ultrashort laser pulse may also increase the harmonic intensity and the order of harmonics generated.

Using the amplifier II output, which may have a fast rise time up to an instantaneous laser intensity higher than $\sim I_s$ in the medium, we tried to observe the higher-order harmonic generation from ions produced through the MPI. The laser intensity was increased to $I \sim 2\times10^{16}$ W/cm^2, but any harmonic radiation higher than the 15th was not observed for He. Note that this laser intensity is sufficiently high for the generation of higher-order harmonics from He ions [9,10]. It was clear that the strong dielectric breakdown destroyed the coherent interaction in the medium and limited the effective laser intensity in the medium to $\sim I_s$ at most, as discussed above. In order that the laser pulse interact with ions before the onset of breakdown, one may require a much higher intensity or a much shorter laser pulse having a faster rise time. This would be the case for the KrF laser experiment [6], where the laser intensity $I \sim 4\times10^{17}$ W/cm^2, much higher than $I_s=(5-6)\times10^{14}$ W/cm^2, was used. Otherwise, a *static* distribution of ions has to be produced temporally prior to the arrival of a fundamental laser pulse, where the laser pulse for the harmonic generation should not modify significantly the temporal and spatial phase relation between the fundamental and harmonic fields. Such an experiment has been made by Akiyama *et al.* [20], where alkali ions were produced by a different laser prepulse and used as the nonlinear medium.

C. Role of the ac Stark effect

It is well known that the plateau itself is a general property of the nonperturbative nonlinear response of an atom to an intense radiation field. In the nonperturbative regime, it has been shown by L'Huillier and co-workers [13,14] that the importance of conventional phase matching is considerably reduced for the harmonic generation, and the harmonic spectrum resembles the single-atom emission.

For comparison with the present experimental results with the single-atom emission with the XeCl laser, we have performed a nonperturbative calculation using the simple model atom proposed by Becker, Long, and McIver [21], where we did not incorporate the MPI. The harmonic distributions calculated for $I \lesssim 1\times10^{15}$ W/cm^2 have neither represented such a plateaulike structure as shown in Fig. 4(a) nor reproduced the characteristic I dependences shown in Fig. 5(a). For example, the calculated 15th-order harmonic in He at $I=1\times10^{15}$ W/cm^2 was weaker than the fifth by several orders. The calculated harmonic distribution has included a rapid decrease in the high-order harmonics, which is similar to that given by the detailed nonperturbative calculations for He at the KrF laser wavelength [10].

The inconsistency between the theoretical and experimental results may be improved by taking into account the ac Stark effect at high intensities. The ac Stark effect is a well-known phenomenon in the above-threshold ionization (ATI) experiments [22], and its role in the high-order harmonic generation has been discussed in detail in

I. Briefly, in an intense radiation field, the excited states and IL of an atom are Stark shifted toward higher energy approximately by a magnitude of the ponderomotive energy E_p given by Eq. (2) [22]. In the ATI experiment done by Perry, Szöke, and Kulander [23], such large shifts of the excited states and IL of He atoms have been observed with intense UV laser pulses, as well as resonance enhancement of the MPI rate due to the shifting excited states.

In the present experiments, the maximum interaction intensity in He is $I \sim 4 \times 10^{14}$ W/cm^2, as discussed above. Then the shift of about 3.5 eV is expected according to Eq. (2). To examine in further detail the possible contribution of the excited atomic states to the high-order harmonic generation, we measured I-dependent harmonic signals in He and Ne. The results for the third-, fifth-, and seventh-order harmonics are shown in Fig. 7. At the lowest intensities in Fig. 7, where the perturbative regime may be still valid, the fifth-order harmonic is most intense in both He and Ne. This is attributed to the fairly large fifth-order nonlinear susceptibilities, because the energy of five 308-nm photons is close to those of the excited states, such as the $2p$ state in He and the $3d$ states in Ne. With an increase in I the fifth-order harmonic is saturated most rapidly, especially in Ne.

This observed characteristic behavior of the fifth-order harmonic can be described by the qualitative model discussed in I. In He, when the ac Stark shift is small at a low intensity, the fifth-order harmonic is generated from the energy region just below the $2p$ (and $2s$) state. With increasing I, the increasing shift of excited states increases the separation between the energy of the five UV photons and the lowest excited-state energy and reduces the fifth-order nonlinear susceptibility or dipole moment. This leads to the rapid saturation of the fifth-order harmonic with an increase in I. On the other hand, at a low intensity the seventh harmonic is generated from the energy region above the IL, and the energy of six 308-nm photons is slightly larger than that of the $5d$ state. With increasing I, the $5d$ and lower excited states shifting to a higher energy region are in transient resonances with the six UV photons. These six-photon resonances can greatly enhance the seventh-order harmonic generation efficiency. The number of excited states in resonance and the resulting enhancement of the seventh increase with increasing I, leading to the maximum at the seventh, as shown in Figs. 4(a) or 7(a).

In Ne, at a low intensity the fifth-order harmonic is generated from the energy region between the closely spaced $3d$ states or ~ 0.08 eV above the $3d[5/2]_3$ state. Even at a low intensity $I \sim 10^{14}$ W/cm^2, several $3d$ and $4s$ substates can cross the five-UV-photon energy, and then the fifth-order harmonic experiences repetitive, large, and rapid refractive index changes during the evolution of a laser pulse and cannot grow up fast with an increase in I, as discussed in detail in I.

The most efficient enhancement due to the transient resonances is expected for the harmonic generated from the energy region just above the *shifted* IL, where the refractive index change due to the shifting excited states would be small. As seen in Fig. 7(b), the seventh harmon-

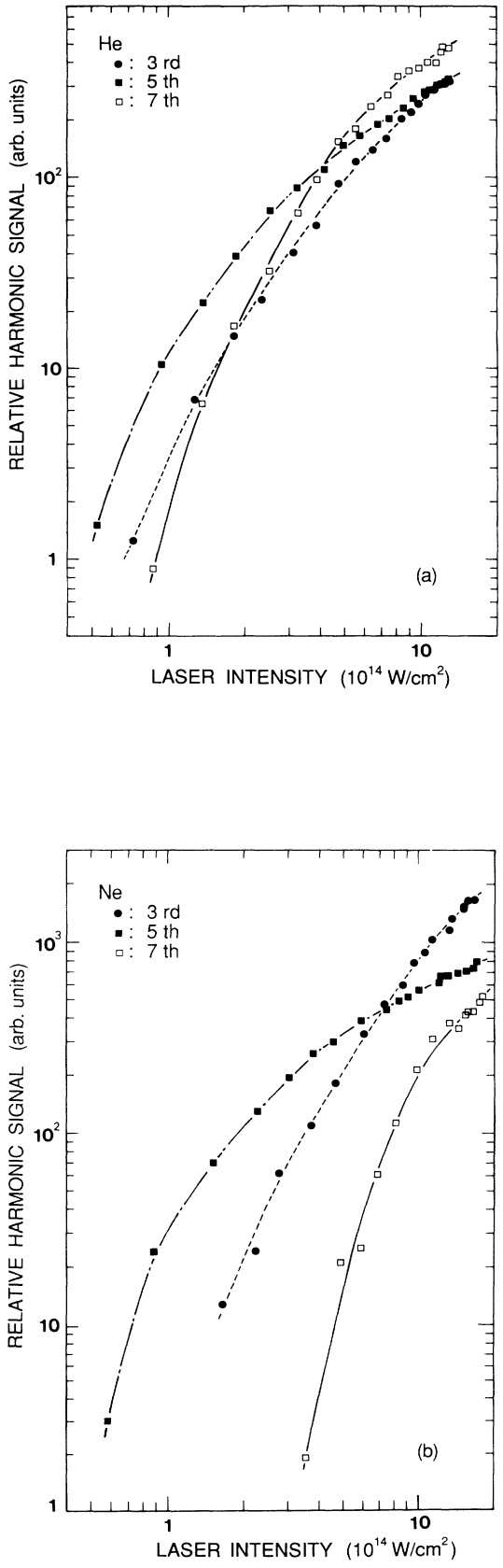

FIG. 7 The third-, fifth-, and seventh-harmonic signals in (a) He and (b) Ne as a function of the XeCl laser intensity.

ic in Ne is generated less efficiently than the third and fifth, although it increases rapidly with an increase in I. For efficient enhancement of the seventh, the six-UV-photon energy (24.15 eV) much larger than the IL (21.56 eV) is required to fall into the energy region below the shifted IL, as discussed above. For this, the shift of the IL or the excited states should be more than ~ 2.6 eV, which is induced at a laser intensity $I \gtrsim 3\times10^{14}$ W/cm^2, according to Eq. (2). However, the saturation intensity I_s for the MPI of Ne atoms is supposed to be much smaller than that ($I_s \sim 4\times10^{14}$ W/cm^2) for He atoms, and such a large shift for the efficient enhancement of the seventh is not expected due to the complete depletion of neutral Ne atoms at a lower intensity than $I \sim 3\times10^{14}$ W/cm^2.

In Fig. 7, the saturation of harmonics at the highest intensity is certainly due to the MPI and subsequent dielectric breakdown of He and Ne atoms. Similarly, in Ar, Kr, and Xe, having much lower energies of the excited states and IL than those of He and Ne, one can never expect efficient high-order harmonic generation due to their larger MPI rates and resulting low thresholds for the dielectric breakdown at the UV.

D. Comparison with the dye-laser results

In I, we reported visible dye-laser experiments, where the highest harmonic orders detected were the 41st in He, the 37th in Ne, the 19th in Ar, the 17th in Kr, and 13th in Xe, and the broad plateaus that were preceded by a minimum at a specific harmonic order were formed in the harmonic distributions, especially for He and Ne. Equation (1) predicts that the highest orders to be observed with the dye laser at $I=1.4\times10^{14}$ and 1.9×10^{14} W/cm^2 are the 19th and 21st for He and Ne, respectively. These harmonic orders predicted are much lower than those observed at the dye-laser intensities. The observed higher-order harmonics also suggest the contribution of the ac Stark shifts of excited state and IL at the high laser intensity, as discussed in detail in I. Recently, Xu, Tang, and Lambropoulos [10] have shown theoretically that the harmonic radiation generated in He with 616-nm radiation is greatly enhanced by the intermediate resonances induced by the ac Stark shifts.

To compare with the results shown in Fig. 7, we measured the I-dependent harmonic signals for Ar and Ne with the visible (616-nm) dye-laser pulses. The results are shown in Fig. 8. At the highest dye-laser intensity $I=2\times10^{14}$ W/cm^2, no dielectric breakdown was observed in Ne, while a weak light flash was often visible in the Ar jet. (The ions were detected even in He at the highest intensity.) Referring to the results of ps-laser experiment for the MPI at ~ 586 nm [24], the saturation intensity I_s for the eight-photon ionization of Ar atoms for the present 616-nm laser is in a range of $I_s=(1-2)\times10^{14}$ W/cm^2. Then, as well as Ne atoms, neutral Ar atoms are expected to survive and interact with the incident laser pulse at the highest intensity in Fig. 8.

As seen in Fig. 8, none of the qth-order harmonic represents a simple dependence of I^q, which is expected in the perturbative regime, where q is the odd integer (harmonic order). The qth harmonic increases much more slowly than the slope of I^q, as expected at the high intensity. This is consistent with the result reported in I, and may support the recent finding of L'Huillier and coworkers [13,14] that the nonlinear polarization proportional to the single-atom response varies much less rapidly in the incident strong field, and the high-order harmonic radiation has an I dependence much weaker than that in the perturbative regime.

In the region of $I \lesssim 3\times10^{13}$ W/cm^2 of Fig 8(a), the higher-order harmonic is weaker and increases more rap-

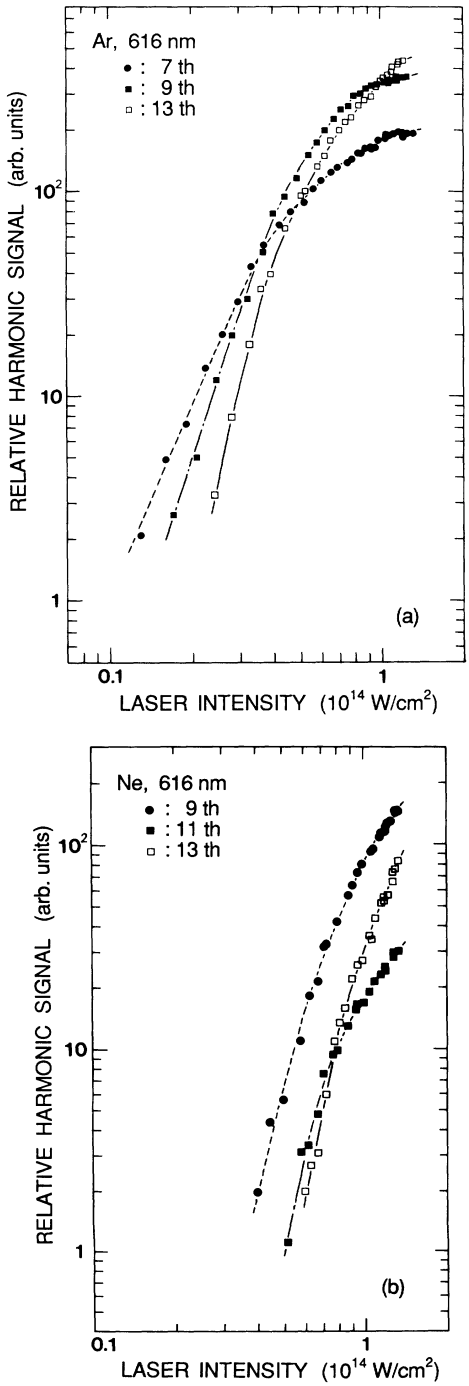

FIG. 8. Harmonic signals in (a) Ar and (b) Ne as a function of the (616-nm) dye-laser intensity.

idly with an increase in I. (Here, we do not note the absolute slope value for the I-dependent harmonic intensity, because we found that the slope was fairly affected by the monochromator slit width and by the focusing position of the fundamental along the optic axis in the nonlinear medium.) With the increase in I, the seventh-order harmonic rapidly decreases the growth rate and begins to saturate first for $I \gtrsim 3\times10^{13}$ W/cm^2. This leads to the formation of a minimum at the seventh in the harmonic distribution observed for Ar (see Fig. 2 in I). The ninth harmonic overcomes the seventh at $I\sim3\times10^{13}$ W/cm^2 and also tends to saturate around $I\sim7\times10^{13}$ W/cm^2. In contrast to these, the 13th harmonic continues to increase rather rapidly with increasing I up to a magnitude comparable to (or higher than) the ninth harmonic, but it also goes into the saturation region at the highest intensities. Note that the harmonic radiation increases and goes into the saturation region in a way characteristic of each order with the increase in I. The saturation at the highest intensity in Fig. 8(a) is certainly due to the depletion of neutral atoms through the MPI.

For Ne having the IL much higher than that of Ar, the highest laser intensity used should be much smaller than I_s for the 11-photon ionization. Therefore the results shown in Fig 8(b) are not influenced very much by the MPI, and the harmonics generated in Ne increase rather rapidly even at the highest intensity. In the harmonic distribution observed for Ne with visible dye-laser pulses, the 11th harmonic has represented a minimum (Fig. 2 in I). In Fig 8(b), as expected, the growth rate of the 11th decreases most rapidly with the increase in I, and the 13th overcomes the 11th to form a plateau preceded by the minimum at the higher intensities.

The characteristic behaviors of the seventh in Ar and the 11th in Ne strongly support the role of the ac Stark shifts of excited states. These specific orders of harmonic are suppressed due to the rapid and large refractive index change induced by the ac Stark shifts of many excited states. At the same time, as discussed in detail in I, the transient resonances of shifting excited states with multiple number of fundamental photons would contribute to the rapid increase in the higher-order harmonics, such as the 13th in Ar and Ne, which are generated from the energy region above the shifted IL.

For heavier atoms, such as Kr and Xe, having a low IL, one cannot expect such an efficient enhancement of high-order harmonics even with the visible laser pulses, because of the same limiting process as with the UV laser. To see this, we made the same measurements as that shown in Fig. 6. An example of the results for Xe is shown in Fig. 9. At $I=2.3\times10^{13}$ W/cm^2, which is smaller than I_s ($\sim3\times10^{13}$ W/cm^2) for the MPI of Xe atoms [25], the ninth harmonic is generated most efficiently when the fundamental is focused into the Xe beam, as expected. At $I=1.4\times10^{14}$ W/cm^2, a strong dielectric breakdown was observed in Xe. Then the laser focus into the Xe beam region is observed to produce a great number of ions due to the MPI and subsequent dielectric breakdown, and a dip of the harmonic signal is formed over the beam region. (In Fig. 9, the ion signal is rather saturated at the peak.) The most efficient generation of harmonics is observed by defocusing the laser pulse from the central region of the Xe beam. This is a similar situation to that observed with the XeCl laser for He and shown in Fig. 6.

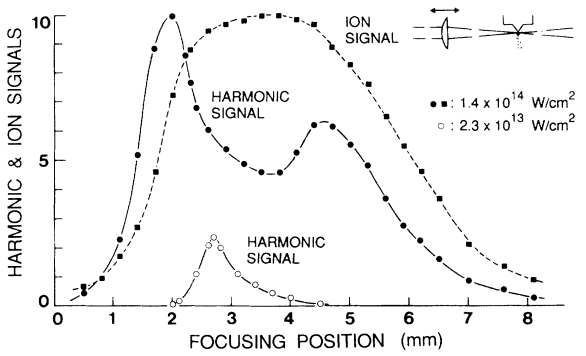

FIG. 9. The ninth-harmonic and ion signals in Xe as a function of position of the (616-nm) dye-laser focus at the intensity $I=1.4\times10^{14}$ W/cm^2 (solid circle and square) and 2.3×10^{13} W/cm^2 (open circle). The maximum harmonic and ion signals are normalized to 10. The confocal parameter $b=8.0$ mm.

In contrast to that for Xe, no dielectric breakdown was observed in He and Ne, even at the highest intensity $I\sim2\times10^{14}$ W/cm^2. For these rare gases, only a single peak of the harmonic signal was observed, of which position coincided approximately with that for the maximum ion signal, when the position of laser focus was moved along the optic axis. This result shows that the MPI itself does not destroy the coherent interaction process for the harmonic generation, as discussed in Sec. III B.

Thus, even with visible dye-laser pulses, the efficient formation of a broad plateau would be restricted for the heavier atoms by the MPI and subsequent dielectric breakdown, which limits the interaction intensity in the medium.

IV. CONCLUSION

We have studied the high-order harmonic generation with sub-ps XeCl laser pulses at high intensities. At the UV, atoms have a relatively large MPI rate and hardly interact with the incident laser pulse at an intensity higher than I_s. The dielectric breakdown that is induced by the free electrons produced through the MPI destroys the coherent interaction for the harmonic generation. The results obtained with the UV and visible laser pulses show that the generation of harmonics in a shorter-wavelength region is possible by using a longer-wavelength fundamental radiation having a shorter pulse width. For such fundamental pulses, atoms have a lower MPI rate and a higher threshold for dielectric breakdown. Furthermore, the longer-wavelength radiation greatly alleviates I, which is required to induce a shift of excited states and IL for the efficient enhancement of high-order harmonics, because of the ω^{-2} dependence of E_p.

ACKNOWLEDGMENTS

The authors would like to thank P. Fons for his critical reading of this manuscript.

[1] M. Ferray, A. L'Huillier, X. F. Li, L. A. Lompré, G. Mainfray, and C. Manus, J. Phys. B **21**, L31 (1988); X. F. Li, A. L'Huillier, M. Ferray, L. A. Lompré, and G. Mainfray, Phys. Rev. A **39**, 5751 (1989).
[2] P. Balcou, C. Cornaggia, A. S. L. Gomes, L. A. Lompré, and A. L'Huillier, J. Phys. B **25**, 4467 (1992).
[3] A. L'Huillier, and Ph. Balcou, Phys. Rev. Lett. **70**, 774 (1993).
[4] J. K. Crane, M. D. Perry, S. M. Herman, and R. W. Falcone, Opt. Lett. **17**, 1256 (1992).
[5] A. McPherson, G. Gibson, H. Jara, U. Johann, T. S. Luk, I. A. McIntyre, K. Boyer, and C. K. Rhodes, J. Opt. Soc. Am. B **4**, 595 (1987).
[6] N. Sarukura, K. Hata, T. Adachi, R. Nodomi, M. Watanabe, and S. Watanabe, Phys. Rev. A **43**, 1669 (1991).
[7] K. Miyazaki and H. Sakai, J. Phys. B **25**, L83 (1992).
[8] J. J. Macklin, J. D. Kmetec, and C. L. Gordon III, Phys. Rev. Lett. **70**, 766 (1993).
[9] J. L. Krause, K. J. Schafer, and K. C. Kulander, Phys. Rev. Lett. **68**, 3535 (1992).
[10] H. Xu, X. Tang, and P. Lambropoulos, Phys. Rev. A **46**, R2225 (1992).
[11] K. Miyazaki, T. Fukatsu, I. Yamashita, T. Hasama, K. Yamada, and T. Sato, Appl. Phys. B **52**, 1 (1991).
[12] H. Sakai, K. Miyazaki, and G. U. Kim, J. Opt. Soc. Am. B **9**, 2015 (1992).
[13] A. L'Huillier, K. J. Schafer, and K. C. Kulander, Phys. Rev. Lett. **66**, 2200 (1991); J. Phys. B **24**, 3315 (1991).
[14] A. L'Huillier, P. Balcou, S. Candel, K. J. Schafer, and K. C. Kulander, Phys. Rev. A **46**, 2778 (1992).
[15] D. R. Miller, in *Atomic and Molecular Beam Methods,* edited by G. Scoles (Oxford University Press, Oxford, 1988), Vol. I, p. 14.
[16] M. R. Howells, in *X-Ray Data Booklet,* edited by D. Vaughan (Lawrence Berkeley Laboratory, Berkeley, CA 1986), Chap. 5.3.
[17] H. Onuki, T. Saito, and H. Okumura, Electrotechnical Laboratory Report, 1987 (unpublished), p. 97.
[18] Ph. Balcou and A. L'Huillier, Phys. Rev. A **47**, 1447 (1993).
[19] Y. P. Raizer, *Laser Induced Discharge Phenomena* (Consultant Bureau, New York, 1977).
[20] Y. Akiyama, K. Midorikawa, Y. Matsunawa, Y. Nagata, M. Obara, H. Tashiro, and K. Toyoda, Phys. Rev. Lett. **69**, 2176 (1992).
[21] W. Becker, S. Long, and J. K. McIver, Phys. Rev. A **41**, 4112 (1990).
[22] R. R. Freeman and P. H. Bucksbaum, J. Phys. B **24**, 325 (1991) and references therein.
[23] M. D. Perry, A. Szöke, and K. C. Kulander, Phys. Rev. Lett. **63**, 1058 (1989).
[24] M. D. Perry, O. L. Landen, A. Szöke, and E. M. Campbell, Phys. Rev. A **37**, 747 (1988).
[25] R. R. Freeman, P. H. Bucksbaum, H. Milchberg, S. Darack, D. Schumacher, and M. E. Geusic, Phys. Rev. Lett. **59**, 1092 (1987).